Aeroelastically adaptive propeller using blades' root flexibility

Y. Sandak and A. Rosen
Faculty of Aerospace Engineering
Technion-Israel Institute of Engineering
Haifa, Israel

ABSTRACT

Usually a fixed pitch propeller is designed to be optimal at cruise speeds. Thus the efficiency is quite low at takeoff or low speeds, as well as during other flight regimes. The present paper shows that by introducing a flexible element into the blade root, the propeller efficiency can be improved over a wide range of velocities. The flexible element reacts to root flap or torsion moments by changing the blade pitch at the root. The root flexibility and the pitch angles at the root at zero loads are chosen such that efficiency will increase during problematic regimes without decreasing the propeller thrust. In the case of straight blades the torsional moment at the root is too small to be used. In the case of swept blades this moment component is significantly increased and can contribute to the design of an optimal aeroelastically adaptive propeller.

NOMENCLATURE

B	number of blades
c	chord
C_l, C_d	cross-sectional lift and drag coefficients, respectively
C_{mac}	cross-sectional aerodynamic moment coefficient (about the aerodynamic centre)
C_T, C_P	propeller thrust and power coefficients, respectively
cf	cost function
d	rotor diameter
$d\vec{F}_I$	force vector that acts on an element of mass of the blade, due to inertia contributions.
dl	length of a blade segment
dL, dD	lift and drag forces that act on a blade segment
dm	mass of an element of the blade.
dM_{ac}	aerodynamic moment that acts on a blade segment
F	Prandtl's tip loss factor.
F_{ax}, F_{ay}, F_{az}	x, y and z components of the aerodynamic force at the blade root
F_{Ix}, F_{Iy}, F_{Iz}	x, y and z components of the inertia force at the blade root
J	propeller advance ratio
j	index of trim points
K_x, K_y	'spring' stiffness at the root
K_0, K_1, K_2, K_3	coefficients in the nonlinear expression for K_y.
M	cross-sectional Mach number
M_{ax}, M_{ay}, M_{az}	x, y and z components of the aerodynamic moment at the blade root
M_{Ix}, M_{Iy}, M_{Iz}	x, y and z components of the inertia moment at the blade root
M_x, M_y, M_z	x, y and z components of the resultant moment at the blade root
n	rotational speed of the propeller in cycles per second
P	power required by the propeller
R	radius of the propeller

Paper No. 2851. Manuscript received 20 August 2003, revised copy received, 17 May 2004, accepted 7 June 2004.

https://doi.org/10.1017/S0001924000000221 Published online by Cambridge University Press

$\vec{R}$	vector distance
Re	cross-sectional Reynolds number
r	radial distance
T	propeller's thrust
V	flight velocity
V_T	tangential component of the rotational velocity seen by the cross-section
V_e	cross-sectional resultant velocity
w	cross-sectional induced velocity
w_a, w_t	axial and tangential components, respectively, of the induced velocity
X,Y,Z	blade root system of co-ordinates
α	cross-sectional angle-of-attack
α_i	cross-sectional induced angle-of-attack
β	cross-sectional pitch angle
ζ	weighting coefficient
η	propeller efficiency.
θ	pitch angle at the blade root.
θ_0	constant pitch angle component at the blade root
θ_s	root pitch angle component due to elastic deformation there.
Λ	sweep angle.
ρ	air mass density.
ϕ	cross-sectional angle of the free incoming flow
$\vec{\Omega}$	propeller angular velocity vector
Ω	propeller angular speed.

1.0 INTRODUCTION

The use of fixed pitch propellers is common in various applications, especially in general aviation, UAVs, ultra-lights, etc. The main advantage of fixed pitch propellers is their simplicity. They are cheap, reliable, light, easy to manufacture and do not require maintenance. However, their use does not offer optimal performance under different flight conditions. In cruise flight, during a dash, or while diving, a higher pitch angle is required because of the increased inflow angle of the blade's cross-sections. If the pitch angle of a fixed pitch propeller is determined such that the propeller will be optimal at cruise, then this propeller will not be optimal during takeoff, initial climb or low speed flight, when a low pitch angle is preferred. If the pitch angle is too large then the blade stalls and the aerodynamic efficiency decreases.

During the history of flight, several techniques were developed[1] in order to adjust the propeller's pitch angle to different flight conditions. During WW2 two-position propellers were used, a low pitch for takeoff and initial climb, and a higher pitch for cruise. Adjustable pitch propellers were also used, enabling preflight setting of the desired pitch position.

The most common technique is the variable pitch mechanism, used especially in constant speed propellers. The control device is a mechanical, hydraulic or electric system, which is rather complicated and not suitable for use in smaller aircraft such as UAVs.

A promising approach to adaptive pitch propellers is based on the blades' flexibility where blade loads twist the blades and change their pitch angle. Such aeroelastic propellers were first used during WW1, when Paragon and Lavasseur wooden S-shaped propellers[1] offered a pitch decrease during takeoff. Over the years[2] the idea of aeroelastic adaptive propellers has been approached in various manners.

Research carried out in 1977[3], pointed out the advantages of using composite blades that twist in response to the loads that act along them. A 5-20% improvement in efficiency was reported. Recently, the Global Company[4] developed composite propellers for general aviation aircraft. These are called Quasi Constant Speed (QCS) propellers. According to the company these propellers have the potential for a 35% reduction in takeoff distance, 40% increase in the rate of climb, and 10% increase in speed.

Although the present paper concentrates on propellers, it is worth mentioning that aeroelastically adaptive blades can improve the performance of other rotary wings. Thus, for example, various researchers investigated the use of aeroelastic tailoring in order to optimize the performance of tilt-rotors. Structural and aerodynamic parameters of tilt-rotors represent a compromise between helicopter and airplane modes. This compromise can be improved by applying aeroelastic tailoring as was shown by[5, 6].

A simple mechanism, allowing variations of the propeller pitch at different flight conditions, may result in important improvements in the performance of UAVs and other aircraft that nowadays use fixed pitch propellers. Regular variable pitch mechanisms are not practical because of increased price, weight and fairly complicated control system.

The present research includes a study on the application of a 'spring like' device, located at the blade root, which reacts to the loads at the root and changes the pitch angle of the blade accordingly. An important improvement in the propeller efficiency is achieved in various flight regimes.

2.0 AERODYNAMIC AND INERTIA LOADS

Aerodynamic and inertia loads act along the blade. The aerodynamic loads define the propeller's performance, namely thrust and torque. Both, the aerodynamic and inertia loads, contribute to the moment at the blade root, and, as a result, to the elastic variation of the blade pitch angle, when an elastic device is placed at the root.

2.1 Aerodynamic loads

The aerodynamic loads are calculated using the vortex theory of propellers[7, 8]. A cross-section of the blade is shown in Fig. 1. V is the flight velocity (axial) of the propeller, while V_T is the tangential velocity that is caused by the propeller's rotation. The induced velocity, w, is comprised of two components: the axial, w_a, and tangential, w_t. The cross-sectional resultant velocity is V_e. The geometric pitch angle of the cross-section, β, is measured from the plane of rotation to the cross-sectional zero lift line. α_i and α are the induced and cross-sectional angles-of-attack, respectively. ϕ is the cross-sectional angle of the free incoming flow. The cross-sectional chord is c.

If a blade segment of length dl is considered, then a lift force dL and a drag force dD act on this segment, as shown in Fig. 1.

Similar to Equation (4.30) of Ref. 7, one obtains:

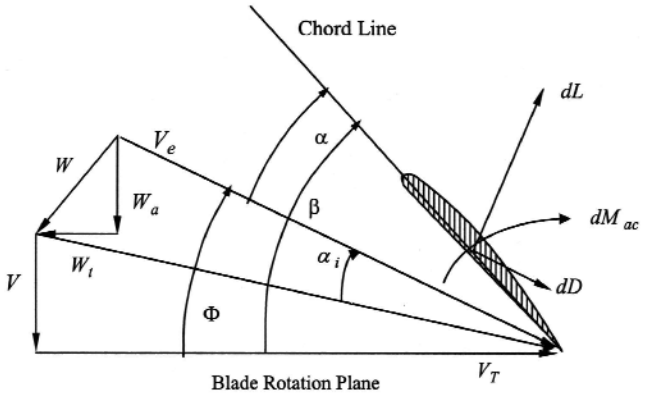


Figure 1. A cross-section of the blade.

https://doi.org/10.1017/S0001924000000221 Published online by Cambridge University Press

$$w_t = \frac{B\,c\,V_e\,C_l(\alpha, M, \mathrm{Re})}{8\pi\,r\,F} \quad \ldots (1)$$

B is the number of blades, r the radial distance of the cross-section, while F is Prandtl's tip loss factor. C_l is the cross-sectional lift coefficient, which is a function of the local angle-of-attack, α, Mach number, M, and Reynolds number, Re. Similar to the derivations of Ref. 7, it can also be shown that:

$$w_a = \frac{1}{2}\left\{-V + [V^2 + 4w_t(V_T - w_t)]^{1/2}\right\} \quad \ldots (2)$$

$$V_e = \left[(V_T - w_t)^2 + (V + w_a)^2\right]^{1/2} \quad \ldots (3)$$

Based on the assumption of a 'two-dimensional' behaviour of each cross-section:

$$\mathrm{d}L = \frac{1}{2}\rho\,c\,V_e^2\,C_l(\alpha, \mathrm{M}, \mathrm{Re})\,\mathrm{d}\ell \quad \ldots (4)$$

$$\mathrm{d}D = \frac{1}{2}\rho\,c\,V_e^2 C_d(\alpha, \mathrm{M}, \mathrm{Re})\,\mathrm{d}\ell \quad \ldots (5)$$

$$\mathrm{d}M_{ac} = \frac{1}{2}\rho\,c^2 V_e^2 C_{mac}(\alpha, \mathrm{M}, \mathrm{Re})\,\mathrm{d}\ell \quad \ldots (6)$$

$C_d(\alpha, \mathrm{M}, \mathrm{Re})$ and $C_{mac}(\alpha, \mathrm{M}, \mathrm{Re})$ are the drag and moment (about the aerodynamic center) coefficients of the cross-sections, ρ is the air mass density.

It should be pointed out that the present analysis includes also the case of swept blades. In this case the cross-section in Fig. 1 is perpendicular to the blade axis and not to a straight radial axis. In such a case the tangential velocity, V_T, is not equal to Ωr, where Ω is the propeller angular speed in radians per second (as in the case of a straight blade), but the influence of the sweep angle should be taken into account while calculating V_T.

At each cross-section along the blade the following parameters are known: r, c, V, V_T, β, F, ϕ and B. The unknowns are: V_e, w_a, w_t, α, α_i, C_l, C_d, dL, dD and dM_{ac}.

The unknowns V_e, w_a, w_t, α, α_i, and C_l are obtained by an iterative solution of Equations (1)-(3), together with the next two:

$$\alpha_i \cong \sqrt{w_a^2 + w_t^2}\,/\,V_e \quad \ldots (7)$$

$$\alpha = \beta - \alpha_i - \phi \quad \ldots (8)$$

In addition the function $C_l(\alpha, \mathrm{M}, \mathrm{Re})$ is also known (in the form of a graph or a table).

After the above six unknowns are obtained, then C_d and C_{mac} are calculated based on graphs or tables: $C_d(\alpha, \mathrm{M}, \mathrm{Re})$ and $C_{mac}(\alpha, \mathrm{M}\ \mathrm{Re})$. Then d$L$, d$D$ and dM are calculated using Equations (4)-(6).

The above iterative procedure is repeated for each cross-section.

The blade is divided into discrete segments. The lift force, drag force and aerodynamic moment acting on each segment are calculated. Since swept blades are considered, two points should be noted:

a. If segment j has a basic pitch angle β_j and a sweep angle Λ_j, then if the pitch angle at the root is changed by θ, the pitch angle of the segment, β_j, becomes:

$$\tilde{\beta}_j \cong \beta_j + \theta \cdot \mathrm{Cos}\,\Lambda_j \quad \ldots (9)$$

At the root there is a zero sweep angle.

b. Due to sweep there is in general a non-negligible flow component along the blade axis. This component results in a friction (drag) force along the axis of the swept part of the blade. This force contributes to the aerodynamic forces and moments that act at the blade root.

A root system of co-ordinates X, Y, Z is defined. This system is attached at the blade root. Pitch variations take place about the X axis, the Z axis points in the axial direction, while Y is the third axis of a Cartesian system.

Now the aerodynamic contributions of all the segments along the blade are summed up to obtain the resultant aerodynamic force and moment at the blade root. Since in general a swept blade is considered (forward and backward sweeps are allowed), the summations are done in an exact vector manner. The aerodynamic force and moment at the blade root are described by their components in the (X, Y, Z) directions, (F_{ax}, F_{ay}, F_{az}) and (M_{ax}, M_{ay}, M_{az}), for the force and moment, respectively.

By a vector addition of the aerodynamic forces and moments of all the blades (the resultant moment is calculated about the propeller disk center), the propeller thrust, T, and power, P, are obtained.

The propeller thrust coefficient, C_T, power coefficient, C_P, and efficiency η, are defined as:

$$C_T = T/(\rho n^2 d^4) \quad \ldots (10)$$

$$C_P = P/(\rho n^3 d^5) \quad \ldots (11)$$

$$\eta = J\,C_T / C_P \quad \ldots (12)$$

where the advance ratio J is:

$$J = V/n\,d \quad \ldots (13)$$

d is the propeller diameter and n the rotation frequency in cycles per second.

The aerodynamic model was verified by comparing its results with experimental results from the literature. For the case of a propeller having straight blades the experiments of Hartman and Biermann[9] were used. For the case of swept blades comparisons with the experimental results of Evands and Liner[10] were performed. In both cases good agreements between calculated and measured results were obtained, thus verifying the aerodynamic model.

https://doi.org/10.1017/S0001924000000221 Published online by Cambridge University Press

2.2 Inertia loads

Consider a small mass element dm of the blade. This element is located at a vector distance $\vec{R}$ from the blade root. The vector of rotational speed of the propeller is $\vec{\Omega}$. Since a 'steady' case is considered here, the only inertia load is due to centripetal acceleration. This force, $d\vec{F}_I$, which acts on the element dm, is obtained after applying D'alambert's principle:

$$d\vec{F}_I = -\vec{\Omega}\times(\vec{\Omega}\times\vec{R})dm \qquad \ldots (14)$$

In order to obtain the resultant inertia force and moment at the blade root, integration is carried out over the entire blade. This integration is divided into integration over the blade cross-section, followed by integration along the blade. Thus the inertia force and moment at the blade root are obtained as integrations, along the blade, of its cross-sectional mass properties. The inertia force and moment at the blade root are described by their components in the X, Y, Z co-ordinate directions: (F_{Ix}, F_{Iy}, F_{Iz}) and (M_{Ix}, M_{Iy}, M_{Iz}), respectively.

2.3 Resultant moment at the blade root

The resultant moment at the blade root is the sum of the aerodynamic and inertia contributions. This resultant is described by its components (M_x, M_y, M_z) where:

$$M_x = M_{ax} + M_{Ix} \qquad \ldots (15a)$$

$$M_y = M_{ay} + M_{Iy} \qquad \ldots (15b)$$

$$M_z = M_{az} + M_{Iz} \qquad \ldots (15c)$$

3.0 DEFINITION OF THE PROBLEM

As indicated above, when fixed pitch propellers are designed to operate in an optimal manner at a certain cruise speed, they are not optimal during take-off, initial climb or low speed flight. In order to present this point more clearly, the two-bladed propeller of [9] is chosen. The pitch angle at the 0·75 radius is 25° and the propeller is rotating at 1,000rpm. This propeller will be used as the basic (nominal) case, which will be studied in the paper. The aerodynamic efficiency of the cross-section at 0·75 radius (a Clark Y profile) is presented in Fig. 2, as the lift to drag ratio of the profile for typical Mach and Reynolds numbers. It should be noted that the angle of attack, α, is measured to the zero lift line of the cross-section. It can be seen that the optimum is obtained at an angle-of-attack of 6-8°. Above an angle-of-attack of 14° the cross-section enters deep stall and the efficiency drops sharply.

In Fig. 3 the angle-of-attack at the representative cross-section (0·75R), as a function of the advance ratio, J, is presented. It can be seen that while the cross-section operates at optimal angles-of-attack near cruise speed ($J \approx 1$), at low speeds the angles-of-attack are above 14°. This trend results in the low efficiency (η) of the entire propeller at low advance ratios, as can be seen in Fig. 4. While for J = 1-1·1 the efficiency is 83%. At advance ratios lower than 0·5 it drops sharply.

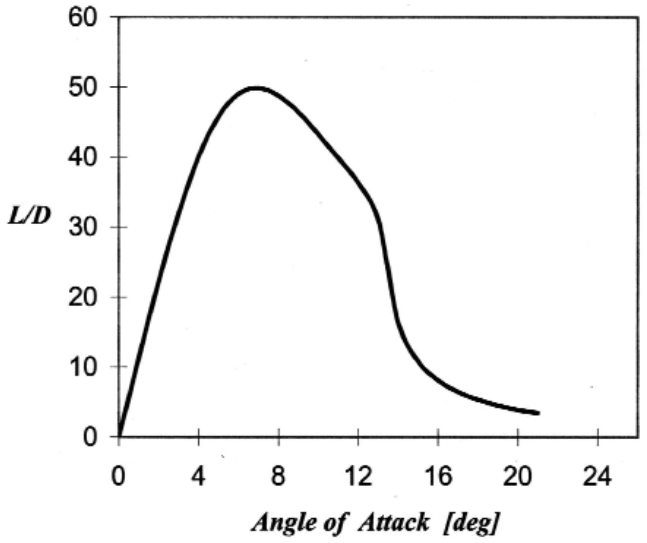


Figure 2. Typical L/D ratio at the 0·75 R cross-section of the blade, as a function of the angle-of-attack.

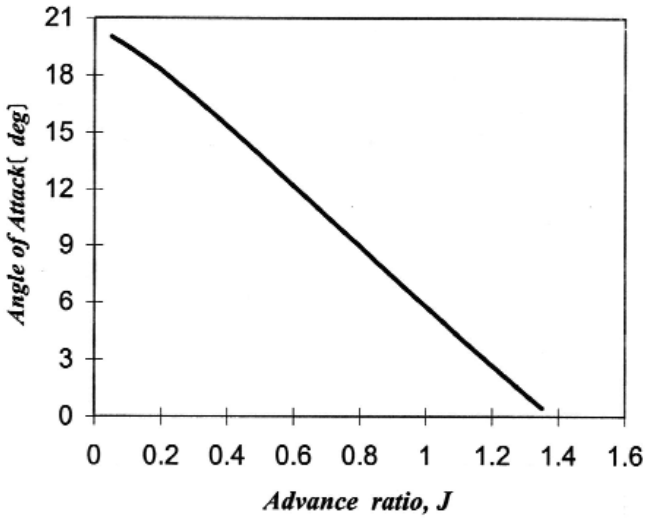


Figure 3. The cross-sectional angle-of-attack at the representative cross-section ($\beta_{3/4}$ = 25°), as a function of the advance ratio J.

Based on the above results it can be concluded that a mechanism, which will result in a decrease in the blade pitch at low advance ratios, will increase the propeller efficiency during takeoff and low speeds.

The idea is to introduce a 'spring like' element into the blade root. This device will react to the moments existing there by changing the blade pitch angle. Since the loads at the root change as a function of the advance ratio, a correct design of the flexible element at the root will result in an increase in the efficiency of the propeller at a predefined range of advance-ratios.

The present investigation is based on the following assumptions:

a. The blade is rigid and thus the cross-sectional pitch angle changes are solely the result of pitch variations at the root.
b. The blade is free from aeroelastic instability problems.

It is assumed that the pitch angle at the root is controlled by the torsional (M_x) and flapping (M_y) moment components there. A positive torsional moment tends to increase the pitch angle, while a positive flapping moment (about the Y axis) tends to deflect the blade into the

https://doi.org/10.1017/S0001924000000221 Published online by Cambridge University Press

direction of flight. Thus the pitch angle at the root, θ, is described by the following equation:

$$\theta = \theta_0 + \theta_s(M_x, M_y) \quad \ldots (16)$$

θ_0 is the pitch angle at the root when $M_x = M_y = 0$. The function represents the "spring like" mechanism at the root.

Since M_x and M_y are functions of θ, the nonlinearity of the problem of calculating the propeller performance increases.

Practically, most of the propellers are designed to operate optimally at cruise speeds. Thus the main purpose of the present investigation will be to increase the efficiency of the propeller at small advance ratios, namely: takeoff, initial climb and level flights at low speeds. From a mathematical point of view the problem concentrates on finding the function, $\theta_s(M_x, M_y)$ which will increase the propeller efficiency at low advance ratios, with a minimal decrease of its efficiency at cruise speeds.

4.0 PROPELLER WITH STRAIGHT BLADES

4.1 Initial studies

Calculations show that in the case of straight blades the torsional moment at the root, M_x, is in general much smaller (more than an order of magnitude) than the flapping moment there. Thus in this case a spring mechanism is used resulting in a pitch angle θ_s, as a function of the flapping moment, M_y. If a linear spring is assumed then Equation (16) becomes:

$$\theta = \theta_0 + M_y / K_y \quad \ldots (17)$$

K_y is the stiffness of the root 'spring'. Its units are (Nm/rad).

In Fig. 4 the propeller's efficiency, η, as a function of the advance ratio, J, for various values of K_y, is presented. The basic case is also presented. As the stiffness of the spring decreases, the efficiency at small values increases significantly, almost without any penalty of a decrease in the efficiency at cruise speeds. In Fig. 5 the variation in the angle of attack at the representative 0·75R cross-section, for the basic case and K_y = 1,000 (Nm/rad), is shown. As a result of the reduction in the value of α, especially at low values of J, the thrust is also reduced significantly. Thus concentration on an improvement of efficiency at low advance ratios is not sufficient. It is necessary to retain thrust in order not to adversely affect the entire aircraft performance. Thus the propeller's designer is faced with a problem of optimization under constraints.

4.2 Optimisation problem

The optimisation problem is defined as follows:
It is desired to optimise the operation of a propeller at N trim points. Each point is defined by its advance ratio J_i, where $1 \le j \le N$. The cost function cf is defined as:

$$cf = \sum_{j=1}^{N} \zeta_j / \eta_j^2 \quad \ldots (18)$$

η is the efficiency of the propeller at the jth trim point. ζ_j are N weighting coefficients.

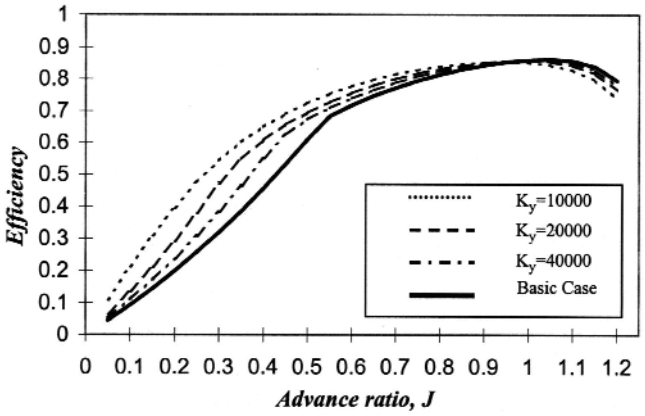


Figure. 4. The effect of a linear spring, K_y, on the propeller efficiency, as a function of the advance ratio.

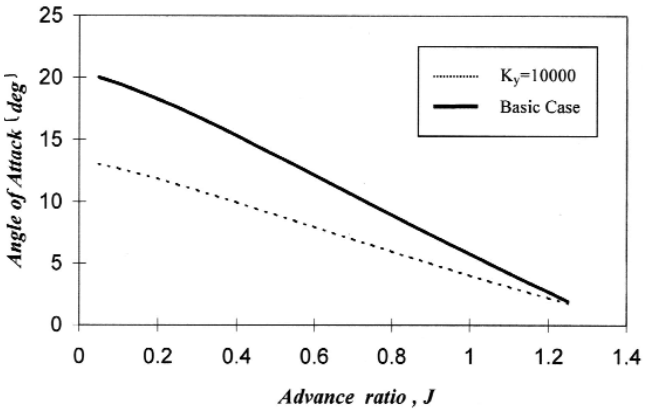


Figure 5. The influence of a spring K_y (1,000Nm/rad) on the angle-of-attack at the 0·75R cross-section.

The result of the optimisation procedure is the definition of θ_0 and the function θ_s of Equation (16), which minimises cf, under the following constraints:

a) At each trim point:

$$C_T \ge 0{\cdot}9\, C_{T\,basic} \quad \ldots (19)$$

where the index basic indicates the value of the variable in the basic (nominal) case.

b) At takeoff and initial climb

$$C_P \ge 0{\cdot}75\, C_{P\,basic} \quad \ldots (20)$$

c) At cruise

$$\Omega = \Omega_{basic} \quad \ldots (21)$$

Condition (b) limits the increase in the rpm at takeoff, to a maximum of approximately 10%.

https://doi.org/10.1017/S0001924000000221 Published online by Cambridge University Press

In all the optimisations to be presented $N = 2$ and $\zeta_j = 1$. The two trim points include:

a) Small J_1, which represents takeoff.

b) A cruise value, J_2.

The values of J_1 and J_2 are obtained from the general design requirements of the aircraft. The optimisation technique is based on SQP (Sequential Quadratic Programming) using MATLAB[11].

The optimisation was executed for the case where θ is defined by Eq. (17). The following data was used:

$J_1 = 0{\cdot}2$
$J_2 = 1{\cdot}0$
$C_T(J_1) = 0{\cdot}1$; $C_T(J_2) = 0{\cdot}043$ (basic)
$C_P(J_1) \geq 0{\cdot}075$

The unknowns are θ_0 and K_y.

An additional constraint in this case is:

$$K_y > 0 \qquad \ldots (22)$$

The optimal solution is:

$$K_y = 18{,}975 \text{ Nm/rad}$$

$$\theta_0 = 0{\cdot}87^\circ \qquad \ldots (23)$$

In Fig. 6 the efficiencies of the basic propeller, a propeller with K_y 10,000Nm/rad and $\theta_0 = 0$ (where the thrust is not kept), and the optimal one (Equation (23)) — are compared. The optimal propeller shows improvements throughout the entire range of advance ratios, especially at the low values. At low values of J the increase in efficiency is not as good as case 10,000Nm/rad and $\theta_0 = 0$, but still at $J = 0{\cdot}2$ there is an increase in efficiency of 8%, and a larger increase of 14% at $J = 0{\cdot}4$. The C_T and C_P values for the three cases are shown in Fig. 7 and Fig. 8, respectively. It is shown that at cruise C_T and C_P of the optimal case are close, as required, to those of the basic case, unlike the case of 10,000Nm/rad and $\theta_0 = 0$. At low advance ratios there is a reduction in the C_P of the optimal case, due to the increase in the rotational speed of the propeller.

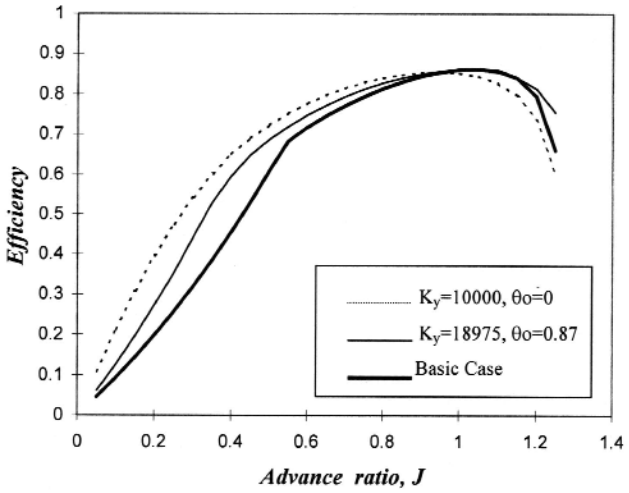


Figure 6. The efficiency for different values of K_y and θ_0.

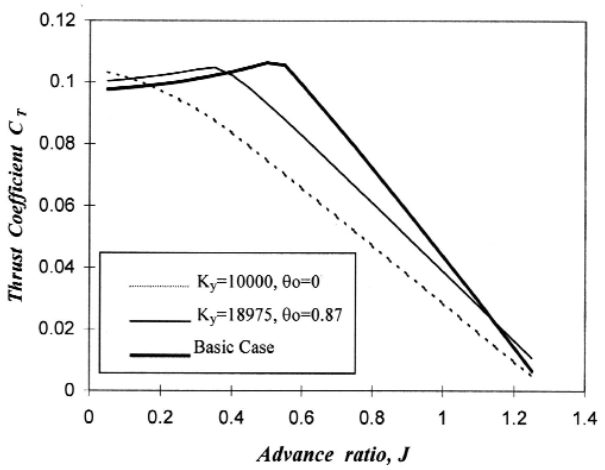


Figure 7. The thrust coefficient for different values of K_y and θ_0.

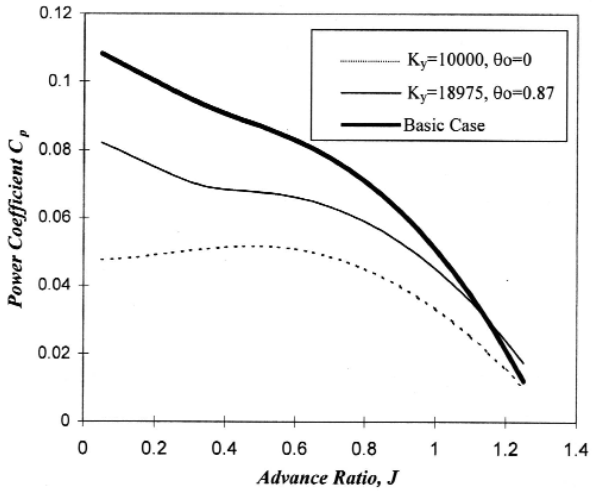


Figure 8. The power coefficient for different values of of K_y and θ_0.

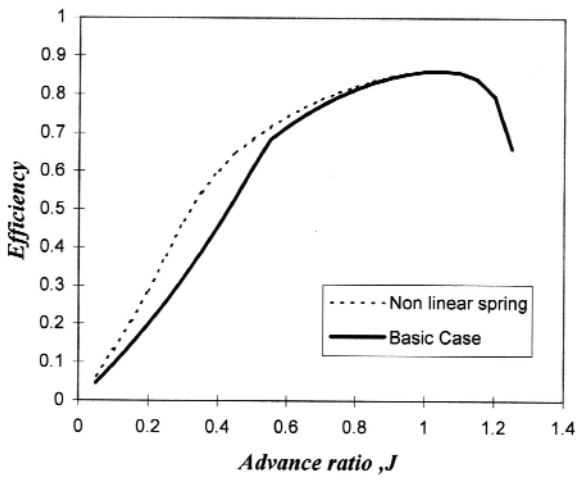


Figure 9. The effect of a nonlinear spring on the propeller efficiency.

https://doi.org/10.1017/S0001924000000221 Published online by Cambridge University Press

4.3 Nonlinear 'spring'

If one examines the previous results it can be concluded that with a mechanism having a constant value of K_y it is difficult to increase the efficiency and retain the thrust at low advance ratios, and at the same time retain the high efficiency at cruise speeds. The solution to this problem is a nonlinear 'spring' mechanism.

One can think of many forms of nonlinear springs. The form that was chosen for the present research includes the following characteristics:

a) The spring is activated only above a certain level of a bending moment M_y (negative or positive). Since negative moments are of interest here, this will be a certain negative value, K_1.
b) At bending moments larger than K_1, a nonlinear cubic spring is activated.

Mathematically this spring is described as follows:

$$\underline{\text{If}} \quad |M_y| \le |K_0| \quad \underline{\text{then}} \quad (\theta - \theta_0) = 0$$

$$\underline{\text{If}} \quad |M_y| > |K_0| \quad \underline{\text{then}} \quad M_y - K_0 = K_1(\theta - \theta_0) + K_2(\theta - \theta_0)^2 + K_3(\theta - \theta_0)^3 \qquad \ldots (24)$$

Optimisation led to the following values:

$$K_0 = -669\,(N \cdot m); \qquad K_1 = 16443\,(N \cdot m)/rad;$$
$$K_2 = 88078\,(N \cdot m)/(rad)^2; \qquad K_3 = 207065\,(N \cdot m)/(rad)^3 \qquad \ldots (25)$$

The improvement in the efficiency of this case, relative to the basic case, is shown in Fig. 9. At high advance ratios the behavior is almost identical to the basic case since an extremely large spring acts there. At low advance ratios there is a very significant improvement in the efficiency without a loss of thrust or a large increase in the propeller rotational speed. At low advance ratios the spring stiffness is slightly reduced.

It is clear that the realisation of a nonlinear spring mechanism is more complicated than a linear one.

5.0 PROPELLER WITH SWEPT BLADES

Propeller blades with swept tips have well known aerodynamic advantages in the case of transonic flow at the tip. In addition, swept blades result in an increase in the torsional moment at the root. This torsional moment can be used to create torsion at the root and consequently a change in the blade's pitch angle. It is clear that the realisation of such a mechanism is simpler than the mechanism that reacts to M_y, since it may involve a simple torsional spring.
In this case Equation (16) becomes:

$$\theta = \theta_0 + M_x / K_x \qquad \ldots (26)$$

In order to investigate the behavior of swept blades, the blades of the basic propeller are swept back by an angle of 37%, from the cross-section at 65% of blade's length, to the tip. This sweep results in an increase of the torsional moment at the blade root by more than an order of magnitude.

Two cases are investigated:

a) K_x = 1,750Nm/rad ; $\theta_0 = 0°$

b) K_y = 1,750Nm/rad ; $\theta_0 = 2°$

These two cases are compared with the basic case.

The thrust coefficient as a function of the advance ratio is shown in Fig. 10. Case (a) results in a decrease in C_T at high advance ratios,

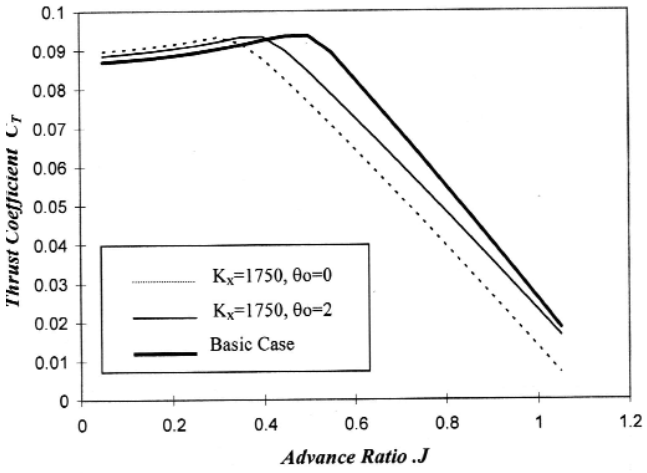


Figure 10. The effect of sweep and a root torsional spring on the propeller thrust coefficient.

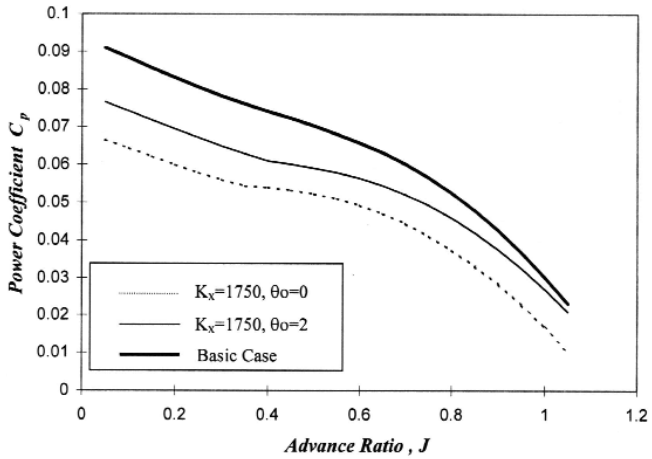


Figure 11. The effect of sweep and a root torsional spring on the propeller power coefficient.

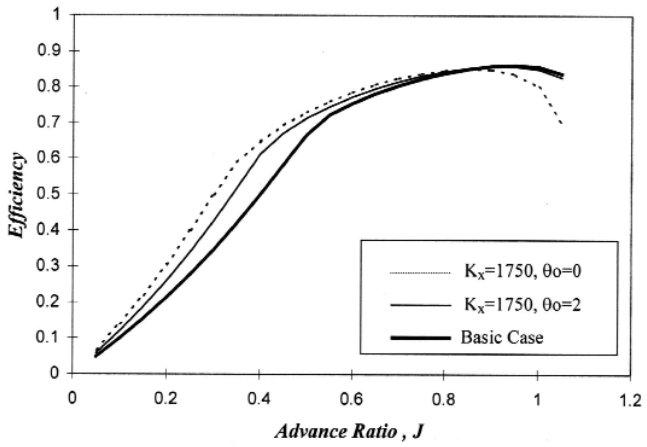


Figure 12. The effect of sweep and a root torsional spring on the propeller efficiency.

https://doi.org/10.1017/S0001924000000221 Published online by Cambridge University Press

while in case (b) most of this decrease disappears. The power coefficient is shown in Fig. 11 and the efficiency is shown in Fig. 12. Case (b) exhibits a significant increase of efficiency at low advance ratios, without a penalty at cruise speeds.

6.0 CONCLUSIONS

The paper presented an aeroelastically adaptive propeller based on a 'spring' element at the blade root. This element reacts to the flap and torsional moments at the blade root and changes the blade pitch angle, accordingly. Since there are different root moments at different flight conditions, it is possible to design the spring such that it will increase the propeller efficiency during problematic flight regimes, with a minimal decrease of efficiency during other regimes.

In the case of straight blades the torsional moment at the blade root is relatively small and thus the flap moment is used as the main driver of the mechanism. The mechanism translates this moment into a pitch variation at the root.

Examples showed that the mechanism investigated might offer efficiency improvements of 7-17%, depending on the specific design of a fixed pitch propeller. In certain cases improvements of more than 20% are also possible. These improvements in efficiency are obtained without hurting the aircraft's performance. Since in many cases propellers are designed to be optimal at cruise speeds, their efficiency during take-off is very poor. Typical aircraft that were studied exhibited a take-off distance reduction of approximately 10%, for a 10% increase of the propeller's efficiency. This improvement at low flight speed may also lead to a 28% increase in the rate of climb.

When blade tips experience high Mach numbers, it is common to sweep them back. In this case the torsional moment at the blade root is increased significantly and so it can be used as part of the adaptive mechanism. Then the mechanism includes a much simpler torsional spring.

The design of the root spring is a typical optimisation problem dependent on many parameters including: aircraft mission profile, engine characteristics etc. The paper concentrated on the investigation of the idea and its potential use, and not on a specific design of the root spring. Yet, it is worth saying a few words about the realisation of the root springs. A possible technique may include regular mechanical devices. But it seems that a more efficient technique will include the use of composite materials, designed to produce, for example, bending/twist coupling in the case of straight blades. Such designs may be similar to the techniques that were suggested for blades of tilt rotors, as mentioned in the introduction.

ACKNOWLEDGEMENT

The authors would like to thank Ms A. Goodman for typing the manuscript.

REFERENCES

1. ROSEN, G. *Thrusting Forward — A History of the Propeller*, 1986, Eastern Press, USA.
2. MUNK, M.M. Propeller containing diagonally disposed fibrous material, United States Patent Office, Patent No 2,484,308, Patented 11 October 1949.
3. DWYER, W.J. and ROGERS, J.B. Aeroelastically tailored propellers, 1977, Society of Automotive Engineering Meeting, SAE Paper No 770455.
4. ANNON Global aircraft puts flexible propeller under test, *Flight International,* 1997, **152,** (4590), pp 25.
5. CHATTOPADHYAY, A., MCCARTHY, T.R. and SEELEY, C.E. Decomposition-based optimization procedure for high-speed prop-rotors using composite tailoring, *J Aircr*, 1995, **32,** (5), pp 1026-1033.
6. SOYKASAP, O. and HODGES, D.H. Performance enhancement of a composite tilt-rotor using aeroelastic tailoring, *J Aircr*, 2000, **37,** (5), pp 850-858.
7. MCCORMICK, B.W. *Aerodynamics of V/STOL Flight*, 1967, Academic Press, New York, pp 73-100.
8. ALJABRI, A.S. Prediction of Propeller Performance and Loading in Uniform and Nonuniform Flowfields, 1978, MSc Thesis, Dept of Aerospace Engineering, Pennsylvania State University.
9. HARTMAN, E.P. and BIERMAN, D. The aerodynamic characteristics of full scale propellers having 2, 3 and 4 blades of Clark Y and RAF6 airfoil sections, 1937, NACA Report No 640.
10. EVANDS, A.J. and LINER, G. A wind tunnel investigation of the aerodynamic characteristics of a full scale swept back propeller and two related straight propellers, 1951, NACA RM L50T05.
11. GRACE, A. *Optimization Tool Box for Use with MATLAB*, 1992, Mathworks, USA.

https://doi.org/10.1017/S0001924000000221 Published online by Cambridge University Press